SUPPLEMENTARY MATERIALS AND METHODS

Electron microscopy

Tg(*mbp*:eGFP) adult fish (sham, 7 dpl and 42 dpl) were terminally anesthetized in 0.1% w/vol Tricaine (Sigma-Aldrich), fixed by injection of modified Karnovsky's fixative (2% glutaraldehyde, 2% paraformaldehyde in 150 mM cacodylate buffer) into the vascular system and kept in fixative for at least 2 hours at room temperature. Fixed spinal cord tissue was then dissected out and kept in fixative at 4°C overnight. Samples were washed twice in cacodylate buffer and twice in water. Samples were postfixed in 2% aqueous OsO_4 solution containing 1.5% potassium ferrocyanide and 2 mM $CaCl_2$ for 30 min on ice, followed by washes in water, incubation in 1% thiocarbohydrazide in water (20 min at room temperature), washed again in water and a second osmium contrasting step in 2% OsO_4/water (30 min, on ice). After several washes in water, the samples were *en bloc* contrasted with 1% uranyl acetate/water for 2 hours on ice, washed again in water, dehydrated in a graded series of ethanol/water up to 100% ethanol, and infiltrated in epon 812 (epon/ethanol mixtures: 1:3, 1:1, 3:1 for 1.5 hours each, pure epon overnight, pure epon 5 hours). Samples were embedded in flat embedding molds and cured at 65°C overnight. To identify the section level of interest (within 50 µm rostral to the lesion site) semithin sections were prepared with a Leica UC6 ultramicrotome using glass knifes and stained with 1% toluidine blue/0.5% borax. Ultrathin sections at the level of interest were prepared using a diamond knife, collected on formvar-coated slot grids and stained with lead citrate (Venable and Coggeshall, 1965). Contrasted ultrathin sections were analyzed on a FEI Morgagni D268 (FEI, Eindhoven, The Netherlands) or a Jeol JEM1400 Plus at 80 kV acceleration voltage.
For the 1 ypl timepoint, the lesion site was not apparent externally and also not visible on the dissected spinal cord itself. To identify the lesion site before targeted ultramicrotomy and TEM analysis, we performed X-ray microtomography (XµCT) on the epon embedded samples, an approach recently developed for several soft tissue samples (Metscher, 2009; Handschuh, 2013; Minarik M, 2017). For the scan, most of the epon around the sample was cut away and the small blocks were glued to the head of a needle. XµCT was performed with the Zeiss XRadia 520 Versa (Carl Zeiss AG, Oberkochen, Germany) using the following parameters: Scan medium: air; Filter: LE1; Optical magnification: 4x; Distance source-sample: 10 mm; Distance source-detector: 25 mm; Exposure time 20 s/image; Number of images: 2950; Binning: 1; pixel size:

0,996 µm. The X-ray scan was reconstructed as a TIFF-stack and the position of the lesion site was determined based on the size of the ventricle along the anterior-posterior axis of the spinal cord. The spinal cords were then remounted on empty epon dummy blocks for ultrathin sectioning. Correct orientation and position of the tissue in the block was controlled several times on toluidine blue/borax stained semithin sections and compared to the corresponding TIFF-stack images of the XµCT scan. Once the lesion site was reached, ultrathin sections were prepared and imaged at the TEM.

Tissue preparation for *in situ* hybridization, immunohistochemistry and CUBIC-based clearing

Adult fish were terminally anesthetized in 0.1% w/vol Tricaine (Sigma-Aldrich) in PBS, fixed by injection of 4% paraformaldehyde solution (PFA) (methanol-free) (Agar Scientific) in PBS into the vascular system and post-fixed in 4% PFA overnight, at 4°C. Fixed tissue was extracted, washed in PBS and either cut in 50 µm-thick transverse vibratome sections (VT 1200S, Leica), 12 µm-thick transverse cryosections (Cryostat HM 560, Microm) or processed whole-mount.

Table S1. Source of *in situ* hybridization probe templates and primers used to generate *in situ* hybridization probe templates.

Gene	ENSEMBL ID	Source	Primer
tnc	ENSDARG00000021948	René Bernitz, CRTD Dresden	-
ctgfa	ENSDARG00000042934	this study	(S) TGTGATTGCTCTGCTGTTCC (AS) GGTGAGGCGATTAGCTTCTG
apoeb	ENSDARG00000040295	this study	(S) ATTACTGACACCATGGCTGAACT (AS) AGTGCTAGTCCAATTGAGTCCAG
sema3c	ENSDARG00000034300	this study	(S) ACGAAAAACATTCATGCCATGGT (AS) GTTGGTAATGGGAGACTGTGTCT

TUNEL cell death assay

Fixed fish were transferred for decalcification and cryo-protection to 20% sucrose/20% EDTA in 0.1 M phosphate buffer pH 7.5, overnight, at 4°C. Fish were further cryo-protected in 7.5% gelatin/20% sucrose in 0.1 M phosphate buffer pH 7.5, at 37°C, frozen in the same solution as a whole and finally sectioned with a rostral to caudal

direction into 12 µm cryosections (Fig. S2). Cryosections were mounted on fat-free superfrost glass slides (StarFrost®, Engelbrecht). For the detection of cell death, the ApopTag Red In Situ Apoptosis Detection Kit (Chemicon), was used according to manufacturer's instructions. A positive (digestion with DNase I (3000-3 U/mL) in 50 mM TrisHCl, pH 7.5, 1 mg/mL BSA) and negative (omitting the TdT enzyme) control slide was included.

Immunohistochemistry

Primary antibodies were mouse monoclonal against PCNA (PC 10, 1:500, Dako); rabbit polyclonal against L-Plastin (custom-made, expression plasmid provided by Michael J. Redd, 1:7500); rabbit polyclonal against Neurofilament 200 (N4142, 1:500, Sigma-Aldrich); rat monoclonal against Claudin K (not commercially available, 1:500, (Munzel et al., 2012)); mouse monoclonal against GFAP (MAB3402, 1:1000, Merck) and chicken polyclonal against GFP (ab13970, 1:3000 and 1:6000, Abcam). For detection, Alexa Fluor® 555 (A21424, 1:750, Invitrogen), Cy™3 (711-165-152, 1:200, Jackson ImmunoResearch Europe Ltd) and Alexa Fluor® 488 (103-545-155, 1:750, Jackson ImmunoResearch Europe Ltd.) conjugated secondary antibodies were used, respectively. Antibodies were incubated in PBS with 0.5% Triton-X. Primary antibodies were incubated overnight at 4°C and secondary antibodies for 2 hours at room temperature.

PCNA staining

To retrieve the antigen for the PCNA staining, vibratome sections were incubated floating in 10 mM Sodium Citrate Buffer pH 6, at 85°C for 20 min. Sections were left to cool down at room temperature, washed with PBS for 10 min and then twice in PBS with 0.5% Triton-X. As the antigen retrieval step quenches endogenous fluorescence when PCNA is used in an endogenously fluorescent transgenic line (i.e Tg(*olig2*:eGFP), an anti-GFP enhancement step was included in the protocol and carried out before (1:3000) and after the antigen retrieval (1:6000).

Tissue clearing

Fixed tissue was washed 3 times for 30 min in PBS with 0.3% Triton-X and then immersed in CUBIC-1 solution overnight, at room temperature. Tissue was thoroughly washed in PBS with 0.3% Triton-X for 3 times for 30 min and immersed in increasing concentrations (vol/vol) of CUBIC-2 solution (25%, 50%, 75% vol/vol in PBS) for 1 hour each and an overnight incubation in 100% CUBIC-1 at room temperature, for final clearing. Tissue was mounted in CUBIC-2 solution in superfrost glass slides (StarFrost®, Engelbrecht) and imaged directly to avoid quenching of endogenous fluorescence. Detection of EdU and nuclear staining with 0.3 µM DAPI (#6335.1, Roth) in PBS took place after incubation in CUBIC-1.

EdU labelling

To monitor cells in the S-phase of the cell cycle after SCI, the 5-ethynyl-2'-deoxyuridine (EdU) nucleoside analog of thymidine (C10340, Invitrogen) was injected intraperitoneally in adult zebrafish at a concentration of 1.25 mg/ml in PBS. Injections started at 5 dpl and took place every 48 hours, for three (Tg(*mbp*:eGFP)) or five (Tg(*olig2*:eGFP)) times. Proliferating cells were detected at 14 dpl with the Click-iT™ EdU Alexa Fluor™ Imaging Kit (Thermo Scientific) according to manufacturer's instructions in either 50 µm-thick vibratome sections or whole-mount tissue after CUBIC-based tissue clearing.

Supplemental Figures

Figure S1

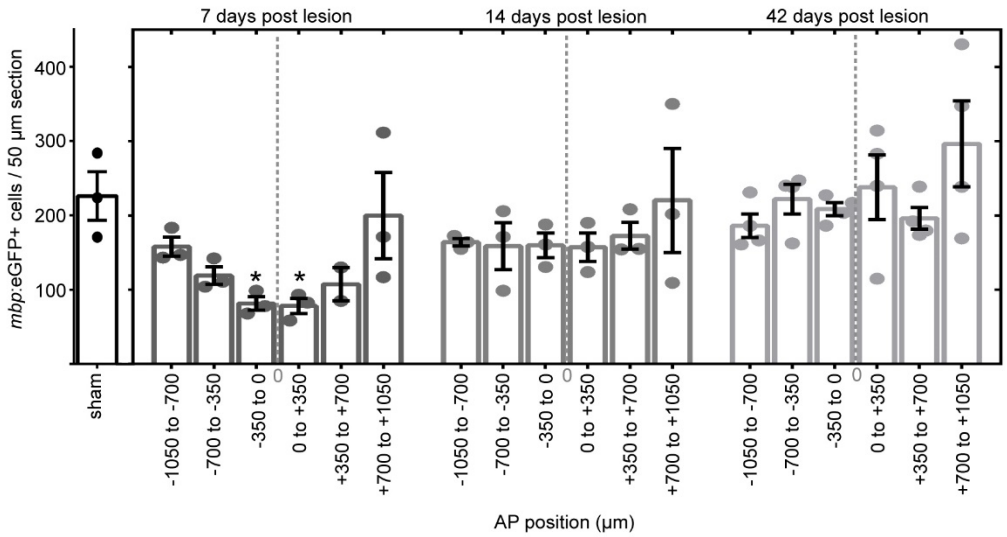

Figure S1. Spinal cord transection results in a spatially restricted loss of mature oligodendrocytes. Stereological quantification of the number of *mbp*:eGFP^{+} somata around the lesion site shows a significant and spatially restricted reduction in the total number of oligodendrocytes at 7 dpl compared to sham controls. Number of experimental animals used were as follows: six for sham control; three for 7 dpl; three for 14 dpl and five for 42 dpl. Data are mean±s.e.m. *P≤0.05 (Kruskal-Wallis followed by Dunn's multiple comparisons post-hoc test). Significance is shown compared to sham control. At 14 and 42 dpl, no significant difference in the number of oligodendrocytes is detected between lesioned and sham control animals. Note that the 7 dpl dataset is the same as presented in Fig. 1C.

Figure S2

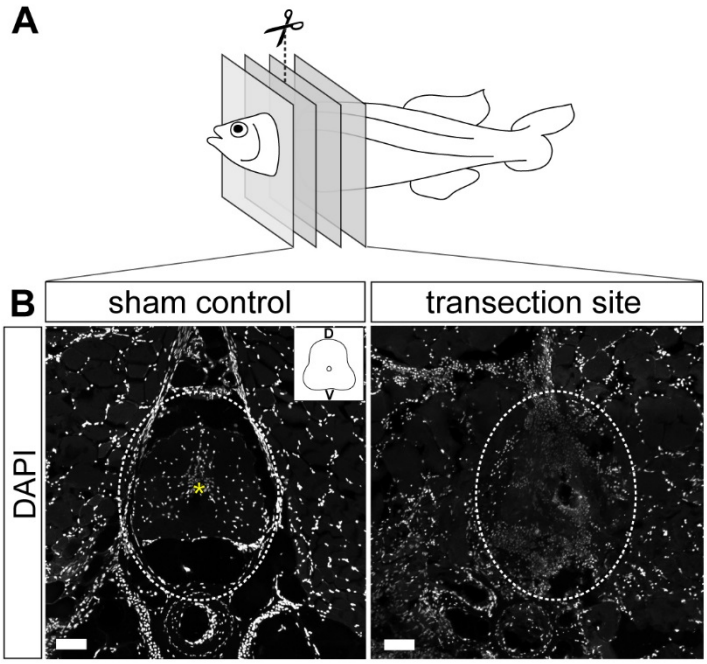

Figure S2. Sample preparation strategy to monitor apoptotic cells in the lesion epicenter. (**A**) After spinal cord lesion, fixed fish are embedded as a whole in cryoblocks and sectioned with a rostral to caudal direction in 12 µm sections. (**B**) Sections are constantly collected until transection site is recognized due to altered tissue morphology. Images shown are maximum intensity projections of transverse sections. D: dorsal; V: ventral. A yellow asterisk indicates the central canal. Scale bars: 100 µm.

Figure S3

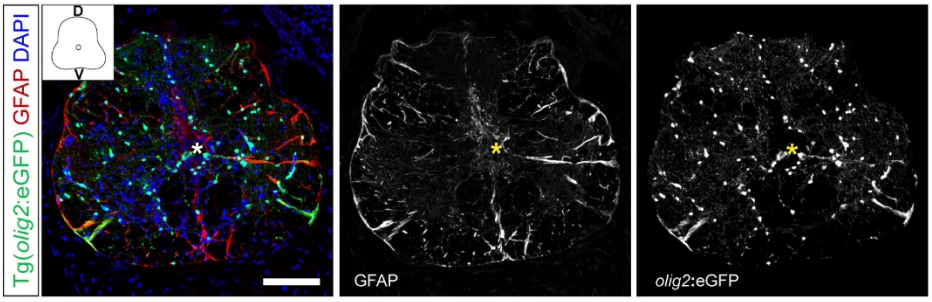

Figure S3. Parenchymal OPCs can be distinguished from *olig2*-expressing ventricular radial glial, based on expression of radial glial markers. In the Tg(o*lig2*:eGFP) line, eGFP is driven by the *olig2* promoter (Shin et al., 2003). In the adult zebrafish spinal cord, *olig2* labels OPCs in the parenchyma and a subset of ventricular radial glia that can be distinguished from parenchymal OPCs based on their size and morphology with long extending processes, markedly lower expression of GFP and expression of radial glia markers ($GFAP^{+}$). Images shown are maximum intensity projections of transverse sections. D: dorsal; V: ventral. In the overview images, a yellow asterisk indicates the central canal. Scale bar: 100 µm.

Figure S4

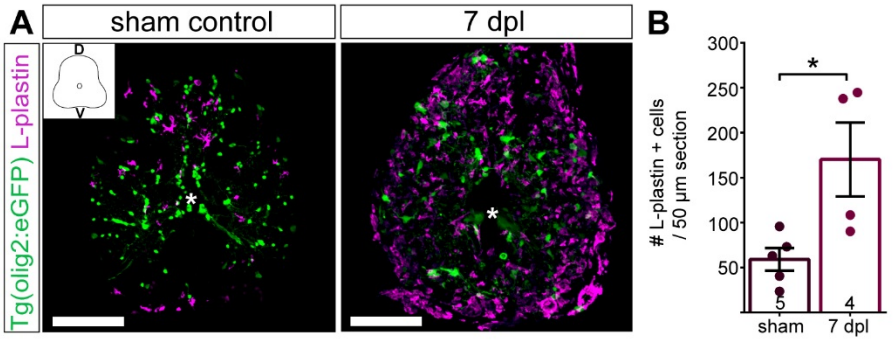

Figure S4. Spinal cord transection results in marked inflammation. (**A**) A marked increase of L-plastin$^+$ cells is detected at 7 dpl. Images shown are maximum intensity projections of transverse sections. D: dorsal; V: ventral. In the overview images, a white asterisk indicates the central canal. Scale bars: 100 µm. (**B**) Stereological quantification of L-plastin$^+$ cells 700 µm around the lesion site shows a significant increase in the number of inflammatory cells at 7 dpl compared to sham controls. Data are mean±s.e.m. Numbers in the plots represent the number of experimental animals. *P≤0.05 (Mann-Whitney test). Significance is shown compared to sham control.

Figure S5

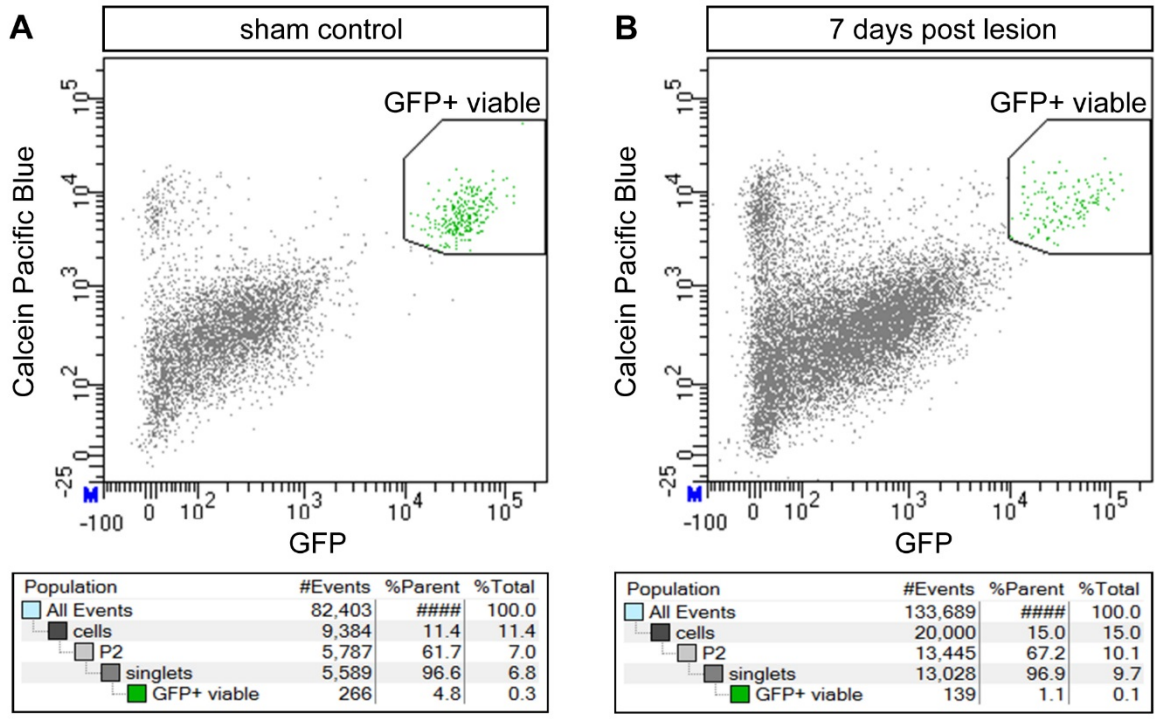

Population	#Events	%Parent	%Total
All Events	82,403	####	100.0
cells	9,384	11.4	11.4
P2	5,787	61.7	7.0
singlets	5,589	96.6	6.8
GFP+ viable	266	4.8	0.3

Population	#Events	%Parent	%Total
All Events	133,689	####	100.0
cells	20,000	15.0	15.0
P2	13,445	67.2	10.1
singlets	13,028	96.9	9.7
GFP+ viable	139	1.1	0.1

Figure S5. Fluorescence activated cell sorting (FACS) of OPCs from ~ 0.5 mm of spinal cord tissue in sham control (**A**) **and 7 dpl** (**B**) **fish.** Gating of OPCs was based on endogenous expression of eGFP and counter stain signal of Calcein Blue AM Dye to sort for viable cells in sham control and 7 dpl groups, respectively**.**

Figure S6

A

Sample	Intragenic		Intergenic	Expression Efficiency	Transcripts	Genes
	Extronic	Intronic				
sham	0,787±0,005	0,114±0,002	0,098±0,003	0,774±0,005	21.223±513,6	10.055±252,3
7 dpl	0,805±0,002	0,104±0,001	0,091±0,001	0,791±0,002	26.904±457,9	12.862±244,1

B

Sample	Total Fragments	Assigned	%
sham	$10.61x10^7$±415.514	$8.226x10^6$±294.066	77,64±0,501
7 dpl	$10.55x10^7$±239.918	$8.404x10^6$±199.449	79,62±0,245

C

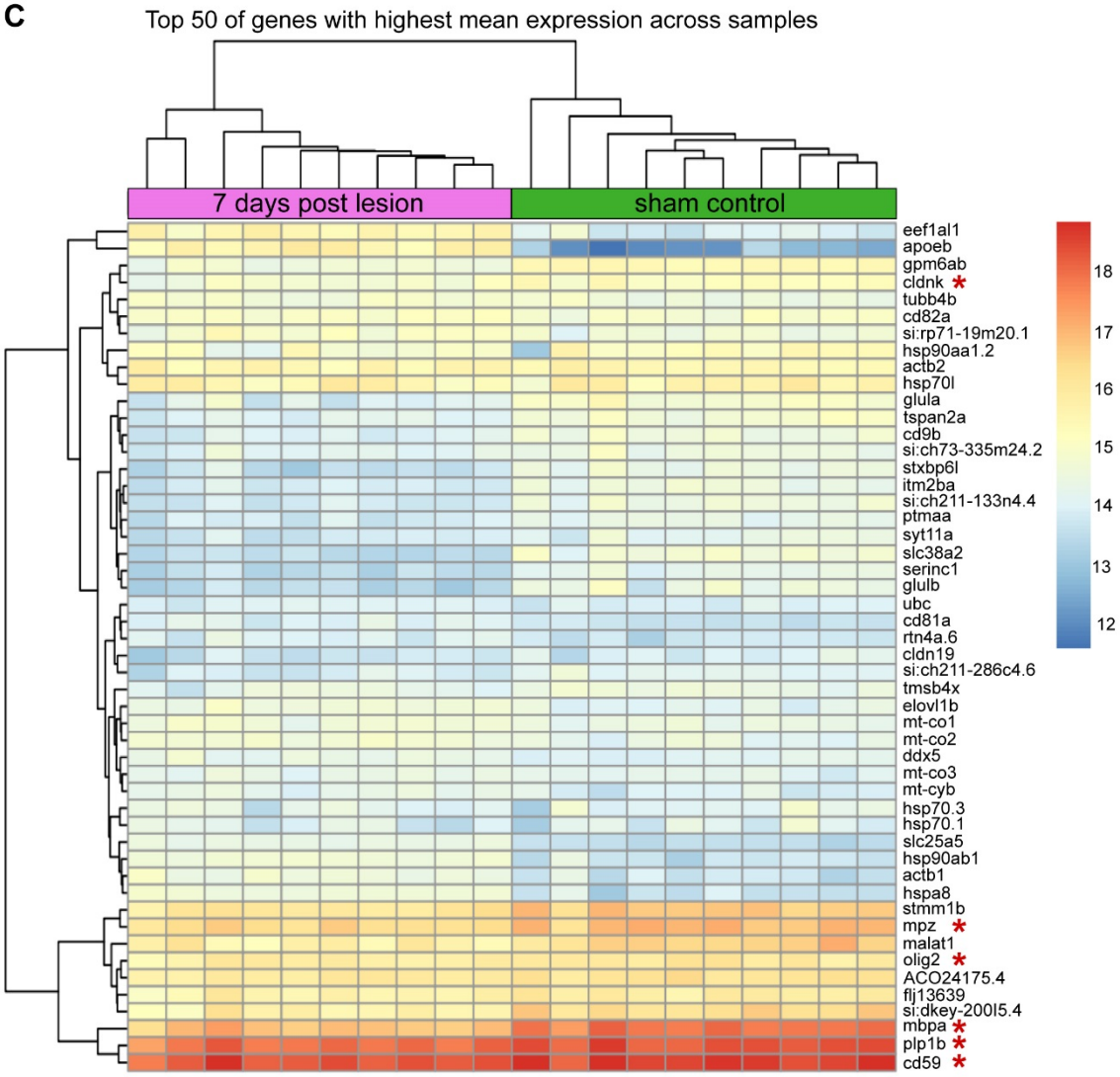

D

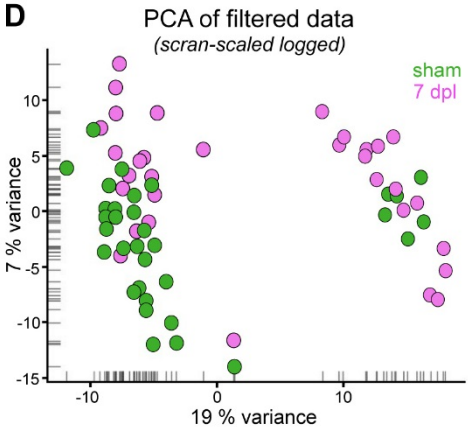

E

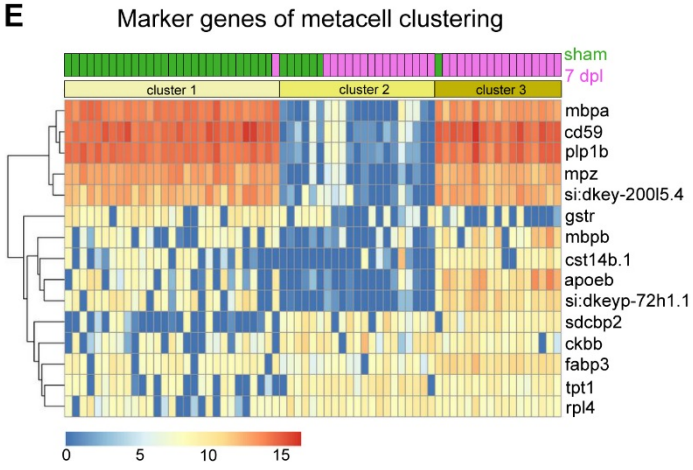

Figure S6. Sample profile, fragment counts and heatmap of genes with highest mean expression across samples (50 genes). (**A**) Sample Profile. The table shows the proportion of reads in exonic, intronic and intergenic regions and the expression efficiency based on the reads in exonic regions. Furthermore, an approximation of the total number of genes and transcripts is provided. (**B**) Fragment Counts. The amount of fragments which are uniquely aligned and within an exonic region is shown (in total number and percentage). (**C**) The normalized fragment counts of the genes are transformed and the mean value across all samples is calculated. This is done for all genes and then the genes with the highest mean are selected. The scale goes from blue to red, with red meaning the highest expression. Typical expected genes for OPCs are indicated with red asterisks. (**D**) Principal component analysis (PCA) of filtered data after single-cell RNAseq of reactive (7 dpl) vs sham control OPCs. Basic gene filtering occurred after filtering mitochondrial genes, rRNA genes and genes with counts in less than 10 cells. Upon filtering, 5,033 genes remained. (**E**) Metacell clustering of differentially expressed genes (DEGs) between reactive and sham OPCs.

Figure S7

Ensemble ID	Gene Symbol	Gene name	log2 Fold Change	*p* value
ENSDARG00000087804	*tnfrsf11a*	tumor necrosis factor receptor superfamily, member 11a, NFKB activator	2.68	0.0007363939
ENSDARG00000056627	*cxcl14*	chemokine (C-X-C motif) ligand 14	8.14	2.483392E-38
ENSDARG00000102583	*il4r.1*	interleukin 4 receptor, tandem duplicate 1	2.21	0.003458611
ENSDARG00000015902	*stat6*	signal transducer and activator of transcription 6, interleukin-4 induced	2.59	0.001042094

Figure S7. Reactive OPCs upregulate genes involved in immune system function. Selection of DEGs involved in immune system function, shown to be upregulated in reactive vs. non-reactive OPCs at 7 dpl.

REFERENCES

Handschuh S (2013) A correlative approach for combining microCT, light and transmission electron microscopy in a single 3D scenario. . Front Zoology.

Metscher DB (2009) MicroCT for developmental biology: a versatile tool for high-contrast 3D imaging at histological resolutions. Developmental dynamics : an official publication of the American Association of Anatomists.

Minarik M (2017) Pre-oral gut contributes to facial structures in non-teleost fishes. Nature.

Munzel EJ, Schaefer K, Obirei B, Kremmer E, Burton EA, Kuscha V, Becker CG, Brosamle C, Williams A, Becker T (2012) Claudin k is specifically expressed in cells that form myelin during development of the nervous system and regeneration of the optic nerve in adult zebrafish. Glia 60:253-270.

Shin J, Park HC, Topczewska JM, Mawdsley DJ, Appel B (2003) Neural cell fate analysis in zebrafish using olig2 BAC transgenics. Methods Cell Sci 25:7-14.

Venable JH, Coggeshall R (1965) A SIMPLIFIED LEAD CITRATE STAIN FOR USE IN ELECTRON MICROSCOPY. The Journal of cell biology 25:407-408.